Cornering Characteristics of the Main-Gear Tire of the Space Shuttle Orbiter

Robert H. Daugherty,
Sandy M. Stubbs,
and Martha P. Robinson

NASA

Cornering Characteristics of the Main-Gear Tire of the Space Shuttle Orbiter

Robert H. Daugherty,
Sandy M. Stubbs,
and Martha P. Robinson

Langley Research Center
Hampton, Virginia

Summary

An experimental investigation was conducted at the NASA Langley Research Center to study the effects of various vertical-load and yaw-angle conditions on the cornering behavior of the main-gear tire of the Space Shuttle orbiter. The parameters measured to evaluate cornering behavior included side force, side-force coefficient, drag force, drag-force coefficient, aligning torque, and overturning torque. The results of the investigation are useful in characterizing the main-gear-tire behavior in flight simulators so that accurate vehicle performance in response to crosswind forces or pilot steering inputs is modeled.

The orbiter main-gear tire was found to behave like most other tires in response to variations in vertical load and yaw angle. The side-force coefficient, which is a measure of cornering efficiency, was found to increase with increases in yaw angle and decrease with increases in vertical load. Drag force was found to increase with increases in vertical load at constant yaw angles. Aligning torque was found to be positive for all conditions tested, a result indicating that the tire is stable in yaw. Overturning torque was found generally to increase with increases in vertical load or yaw angle.

Introduction

The Space Shuttle orbiter is the first spacecraft of its kind intended to land on conventional landing gear and runways. This kind of mission flexibility requires the vehicle to operate in a variety of environments and conditions, and thus factors affecting the handling qualities of the vehicle need to be fully understood. The response of the orbiter tires to crosswind forces and steering inputs greatly influences the way that the vehicle handles on the runway. Previous studies have documented the cornering behavior of the orbiter nose tires under simulated operating conditions (ref. 1). To aid further in the understanding of vehicle performance on the runway, a study of the main-tire cornering behavior was performed. Road-wheel dynamometer studies have been conducted on the main tires, but these tests were performed mainly to examine tire carcass strength. When these tests are used to examine cornering behavior, however, the data are usually incorrect because of the surface texture and rubber contamination of the steel drum used to roll the tire on.

The purpose of this paper is to present the results of tests conducted at the Langley Aircraft Landing Dynamics Facility (ALDF) to determine the cornering characteristics of the main tires of the Space Shuttle orbiter under simulated flight conditions.

The characteristics include side force, side-force coefficient, drag force, drag-force coefficient, aligning torque, and overturning torque. Data were generated for yaw angles ranging from 0° to 10° and for vertical loads ranging from approximately 15 000 to 122 000 lb. Test speeds ranged from approximately 5 knots (for towing tests) to 224 knots (the maximum speed of the test facility). These parameters cover the full range of load, yaw-angle, and speed conditions expected during orbiter landing operations.

Symbols

All values for parameters in this report are presented in U.S. Customary Units.

D	distance between vertical beams (or drag beams)
F_d	total drag force parallel to wheel plane, lb
$F_{d,n}$	drag force measured on north side of tire, lb
$F_{d,s}$	drag force measured on south side of tire, lb
F_s	side force perpendicular to wheel plane, lb
F_z	total vertical force on tire, lb
$F_{z,n}$	vertical force measured on north side of tire, lb
$F_{z,s}$	vertical force measured on south side of tire, lb
M_x	overturning torque, ft-lb
M_z	aligning torque, ft-lb
R	load ratio
β	coefficients of curve-fitting equations
μ_d	drag-force coefficient parallel to wheel plane
μ_s	side-force coefficient perpendicular to wheel plane
ψ	tire yaw angle, deg

Abbreviation:

KSC	Kennedy Space Center

Apparatus and Test Procedure

Test Tires

The tires used in this study were 44.5 × 16.0—21 bias-ply aircraft tires with a 34-ply rating. A

photograph of a new tire is shown in figure 1. The tires have a 5-groove tread pattern made of natural rubber with the grooves 1/10-in. deep. The tires have 16 actual carcass plies and their rated load and inflation pressure are 60 900 lb and 315 psi, respectively. All tests were conducted at this inflation pressure.

Test Facility

All tests in this investigation were conducted at the Langley Aircraft Landing Dynamics Facility (ALDF). The facility consists of a set of rails 2800 ft long on which a 60-ft-long, 108 000-lb carriage travels. A photograph of the facility is shown in figure 2. The carriage is propelled at speeds up to 224 knots by a high-pressure water jet and is arrested by a set of water turbines connected by nylon tapes. A more detailed description of the facility can be found in reference 2.

Tires were mounted on one of two main wheels of the Space Shuttle orbiter, and an existing axle was modified to allow the wheel and tire to be mounted in the dynamometer, which is described below. Brass lugs were designed to simulate the polar moment of inertia of the rotating portion of the actual brake and were installed in the wheel.

Tests were conducted on both a smooth concrete surface and a concrete surface simulating the runway at the NASA Kennedy Space Center (KSC). The simulated runway, shown in figure 3, was an extremely rough surface with 1/4-in-wide by 1/4-in-deep grooves cut transverse to the direction of motion and spaced on $1\frac{1}{8}$ in. centers. The average texture depth was 0.004 in. for the smooth runway surface and 0.03 in. for the rough runway surface. The average texture depth of a surface is determined by spreading a known volume of grease on the desired surface and then measuring the area it covers. A detailed description of the technique can be found in reference 3. In all tests, the runway surface was level and dry.

Instrumentation

The parameters measured in this study included tire vertical load, side load, and drag load. These forces were measured by using the dynamometer that is pictured and sketched in figure 4. Vertical load was measured by using two separate strain-gauged beams, and variations in their load distribution provided a measure of overturning torque. Likewise, drag load was measured by using two separate instrumented beams, and variations in their load distribution gave a measure of aligning torque. Side load was measured using a single instrumented beam mounted in line with the wheel axle. A three-axis accelerometer package was mounted directly to one end

of the wheel axle to permit the acceleration forces of the lower mass to be isolated from the tire-contact-plane force data in all three axes. The lower mass is the effective mass that the load beams support and includes the mass of the axle, wheel, tire, and part of the dynamometer itself. The acceleration data assure that final calculations of loads data represent the forces generated only by the tire.

Analog data from each transducer were converted to digital signals onboard the carriage by the pulse-code-modulation system and were serially telemetered to a receiving station where the data stream was decommutated. This set of data remained in digital form and was fed into a desktop computer. The same set of data was also passed through a digital-to-analog converter and fed through a 14-channel frequency-modulated tape recorder; ultimately, the data were reproduced by a 14-channel oscillograph to give an immediate accounting of carriage and transducer performance during a run. The telemetry system is capable of providing a 200-Hz response. The digital signals transmitted from the carriage permitted a data resolution of 1 part in 256. Normally, full-scale span on each channel was approximately 75 percent of the maximum, thus resulting in a resolution of the system of approximately 0.5 percent.

Test Procedure

The test procedure consisted of rotating the dynamometer and wheel assembly to the desired yaw angle, accelerating the carriage to the desired speed, lowering the tire, applying the preselected vertical load, and recording the output from the transducers. The yaw angles tested were $0°, 1°, 2°, 4°, 7°$, and $10°$. Some runs were conducted at speeds up to 224 knots, whereas others were conducted using a tug to tow the carriage at walking speeds. Normally, a vertical load of approximately 70 000 lb is the maximum capability of the test carriage; however, for tests using vertical loads up to approximately 122 000 lb, approximately 50 000 lb of dead weight was added to the carriage before tow tests were conducted. This configuration is shown in figure 5.

Data Reduction

During a run, the digital data received from the carriage are recorded by the desktop computer at a rate of 1600 samples per second. Typically, force and acceleration data are retrieved from the computer memory at a rate of 400 samples per second and then mathematically filtered to 30 Hz. As stated, vertical load was obtained by adding the outputs of two load beams, and it was then corrected using axle acceleration data to account for lower mass inertial effects. Side force and drag force were obtained in

a similar manner. The side-force coefficient μ_s was defined by the relationship

$$\mu_s = F_s/F_z$$

and the drag-force coefficient μ_d was defined by the relationship

$$\mu_d = F_d/F_z$$

Aligning torque M_z was defined by
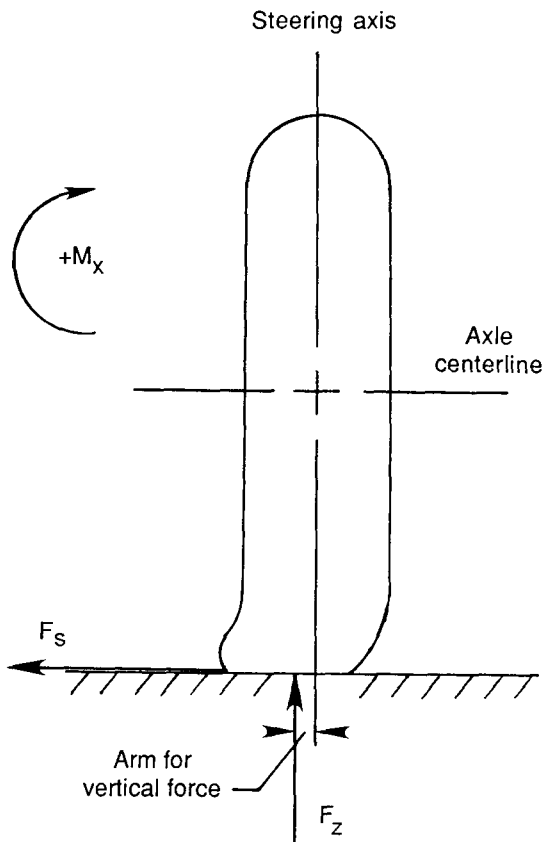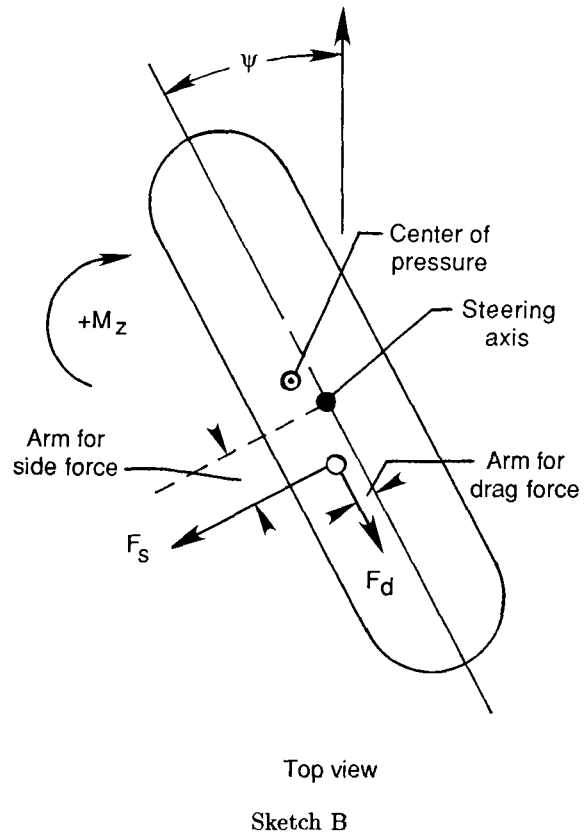
$$M_z = \left(F_{d,n} - F_{d,s}\right)D$$

Overturning torque M_x was defined by

$$M_x = \left(F_{z,n} - F_{z,s}\right)D$$

Load ratio R was defined by

$$R = F_z/60\,900$$

Sketches A and B, which are drawn showing positive sign conventions, display the forces and torques acting on a yawed rolling tire.

Top view

Sketch B

Rear view

Sketch A

Results and Discussion

Data gathered during 19 tests are presented in table I. Listed for each run are one or more vertical-load and yaw-angle conditions along with the associated drag force and side force, drag-force and side-force coefficients, and overturning and aligning torques. The vertical load is also expressed by the parameter R which is the ratio of vertical load to the rated load of 60 900 lb. One should note that the rated load for a tire is that load which produces approximately 35 percent deflection at the rated inflation pressure. Although R is a nondimensional value, it cannot be used to compare characteristics between two different tires. For example, one cannot expect the orbiter nose-gear tire to produce the same side-force coefficients as the orbiter main-gear tire even though their yaw angles and R values may be identical. Results reported in references 1 and 4 indicate that on dry concrete, tire-contact-plane forces and moments are normally insensitive to variations in speed. All the main-tire data were found to be insensitive to variations in speed as well, but for completeness speed is presented in table I for each run. All tests reported in the main body of this report were conducted

on a dry concrete runway. Limited tests on other surface types under wet and dry conditions were also conducted, and the results are presented in the appendix.

All data are presented in the form of carpet plots to show the behavior of each parameter as a function of vertical load (R) and yaw angle. Each carpet plot shows the measured data points from table I and the result of a least-squares bicubic curve fit to the test data. The carpet plots show lines of constant load and yaw angle to aid the reader. Note that these carpet plots represent three-dimensional data surfaces projected onto a two-dimensional surface. Table II presents the coefficients of bicubic interpolation. The following paragraphs discuss the effects of vertical load and yaw angle on the cornering characteristics of the main-gear tire of the Space Shuttle orbiter.

Side Force

The effects of vertical load and yaw angle on the side force produced by the tire are shown in figure 6. The side force F_s is perpendicular to the wheel plane; therefore, to determine the effect of side force on vehicle handling, one would have to translate the force into a cornering force that acts normal to the direction of motion. The plot in figure 6 shows that increasing the value of R while holding the yaw angle constant increases the side force up to a point where R is equal to between 0.75 and 1.50. The data show that the tire is literally load limited in terms of side force to a point where further increases in vertical load actually reduce the magnitude of the developed side force. At low values of R, side force increases with yaw angle until a peak is reached, and thereafter increases in yaw angle cause the side force to be reduced.

The side-force data are also shown in figure 7 in the form of side-force coefficient, which is simply the side force normalized by the vertical load on the tire. This coefficient can be used to express the efficiency of the tire in producing side force. The figure shows in general that for any load condition, increases in yaw angle produce increases in the side-force coefficient. The only exception to this occurs at values of R of 0.75 and less with the yaw angle greater than 7°. The plot also shows that for a given yaw angle, increases in vertical load result in a decrease of the side-force coefficient or efficiency in side-force development. These results are similar to those reported in references 1 and 4.

Drag Force

The effects of vertical load and yaw angle on the drag force produced by the tire are shown in figure 8.

The plot shows that while a constant yaw angle is maintained, increasing the values of R produces increased drag force. For constant values of R up to approximately 1.00, increasing the yaw angle results in a relatively flat curve plot. Increasing the yaw angle at constant loads appears to have a larger effect on increasing the drag force for load ratios greater than 1.00 than less than 1.00. This result may be due in part to the excessive tire deflections at these loads.

The drag-force data are also presented as drag-force coefficient in figure 9. This parameter is derived in the same manner as the side-force coefficient. Figure 9 shows a concentration of the experimental data and the curve fit in the region of a drag-force coefficient of 0.02 for low yaw angles and all loads. This indicates that 0.02 represents the rolling resistance (or deceleration) of the basic tire. Note that none of the data are resolved into increments smaller than a drag-force coefficient of 0.01 since it is unrealistic in practice to make more accurate measurements. Agreement of the curve fit with these data is not sufficient to draw logical conclusions of the behavior of this parameter throughout the range of the conditions tested.

Aligning Torque

Aligning torque is the torque developed by a yawed-rolling tire that tends to return the tire to a zero-yaw condition. Consequently, negative aligning torque indicates an unstable condition. Aligning torque is the sum of two torques. One is the torque developed by the side force acting behind the steering axis. The other is torque due to the drag force acting through a laterally shifted center of drag and side force. The forces and arms depicting these torques can be seen in the sketches in the data reduction section of this report. Figure 10 shows the response of aligning torque to variations in yaw angle and load ratio. The plot shows that increases in load at a constant yaw angle generally increase the aligning torque. At loads corresponding to $R = 0.50$ and less, changes in aligning torque are small for changes in yaw angle. These data also indicate that the aligning torque reaches a maximum for all load conditions, and that these maximum values occur at a higher yaw angle as the load is increased.

Overturning Torque

Overturning torque is the torque developed by a yawed-rolling tire that tends to tilt the wheel plane away from vertical. Overturning torque is the sum of two torques. As can be seen in sketches A and B shown earlier, one torque is produced by the side force acting through the axle-to-ground distance, and

the other torque is produced by the tire vertical load acting through a laterally shifted center of pressure. Figure 11 shows a carpet plot of overturning torque as a function of yaw angle and load ratio. The figure shows that holding the yaw angle constant and increasing the vertical load causes the overturning torque to increase up to loads corresponding to about $R = 1.50$. Thereafter, slight decreases are seen in the overturning torque up to $R = 2.00$. Holding a constant vertical load and increasing the yaw angle causes the overturning torque to increase except for loads corresponding to $R = 0.50$ or less at yaw angles greater than 7°. Slight decreases in the overturning torque are seen in this region of low vertical load and high yaw angle.

Concluding Remarks

An experimental investigation was conducted to examine the cornering characteristics of the main-gear tire of the Space Shuttle orbiter. Data were obtained at the Langley Aircraft Landing Dynamics Facility at tire yaw angles up to 10° and at loads up to approximately 122 000 lb. These conditions span the range of conditions likely to be experienced in flight operations. The cornering characteristics were evaluated by examining parameters such as side force, side-force coefficient, drag force, drag-force coefficient, aligning torque, and overturning torque.

The results of the investigation indicated that the tire behaves in a manner similar to that of other tires in that the side-force coefficient, or efficiency, basically increases with yaw angle and decreases with vertical load. Previous tests have shown similar tire cornering behavior to be insensitive to variations in speed on dry concrete surfaces, and this was determined to be true for the orbiter main-gear tire as well. Drag force was found to increase as vertical load was increased at a constant yaw angle. At high loads, increasing the yaw angle was found to increase the drag force.

Aligning torque developed by the tire is positive for virtually all conditions tested, an indication that the tire is stable in yaw for all expected flight conditions. Overturning torque generally increases with increasing yaw angle or increasing load.

Appendix

Effect of Surface Type and Wetness Condition on Side-Force Coefficient

As part of a separate series of tests to examine the wear characteristics of the main-gear tire of the Space Shuttle orbiter on various surface types under wet and dry conditions, data were produced to allow comparisons of side-force coefficient on various surface types and conditions to be made.

Figure A1 shows such a comparison for a tire yaw angle of 4° and a vertical load of approximately 55 000 lb. The tire pressure was 315 psi for all conditions and the speed for each test was approximately 200 knots. All surfaces were tested both wet and dry, and the wetness condition for each surface was representative of a recently passed rain shower. For example, after wetting, each surface was more than damp, but no puddles were present. Figure A1 shows that a side-force coefficient between 0.27 and 0.28 was developed on the KSC surface (highly textured and grooved) regardless of its wetness condition.

The KSC surface was painted with runway paint (coverage was 100 ft^2/gal) as shown in figure A2, and tests were conducted on it. The dry-condition side-force coefficient was about 0.26, although the coefficient dropped to approximately 0.14 when the surface was wet.

Figure A3 shows the KSC surface after sandblasting. The texture of the surface was greatly reduced, and the corners of the land areas near the grooves were highly rounded. Tests on this surface showed a decrease in the dry performance compared with that on the untreated KSC surface, thus yielding a side-force coefficient of about 0.22. When wet, a side-force coefficient of 0.16 was obtained. Finally, tests were conducted on a smooth concrete surface without grooves. The average texture depth on this surface was 0.004 in. The side-force coefficient on this surface was 0.25 when dry and was reduced to about 0.06 when wet.
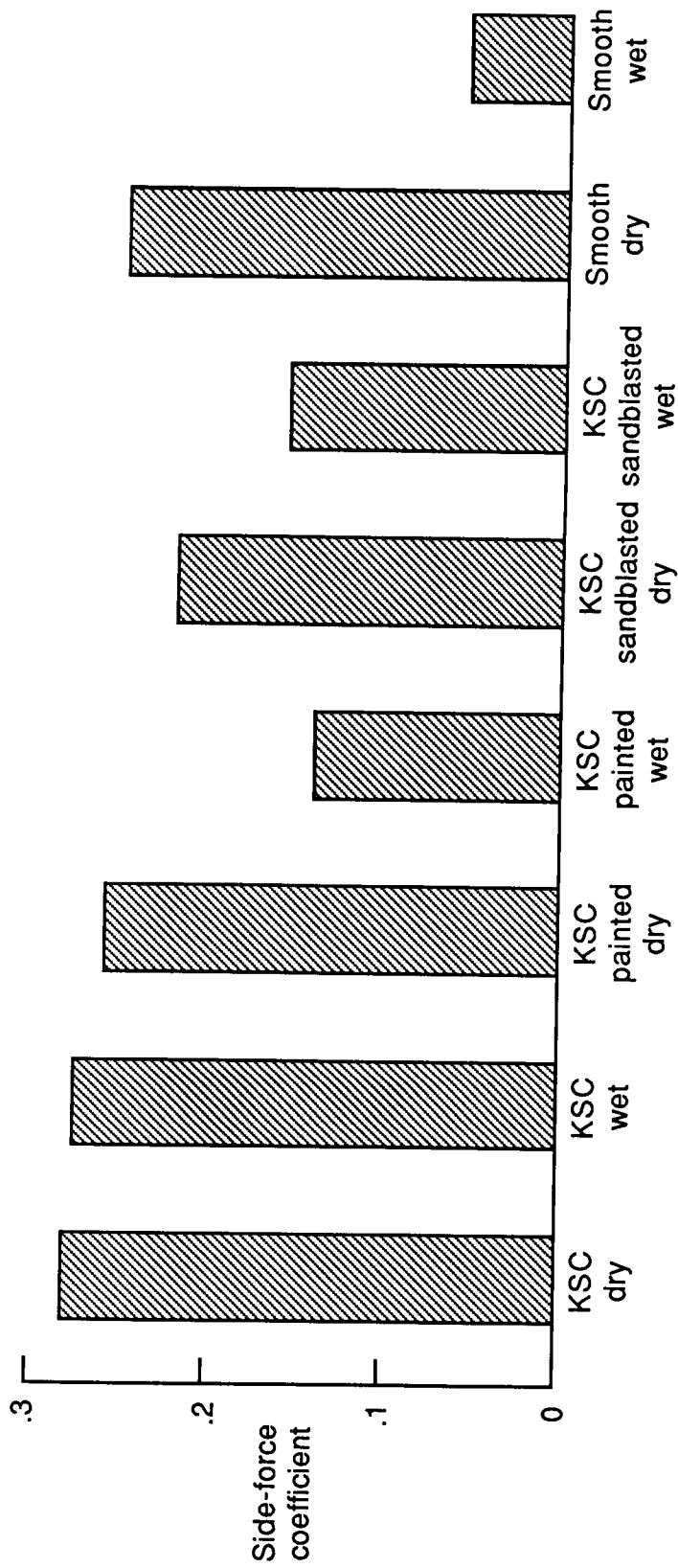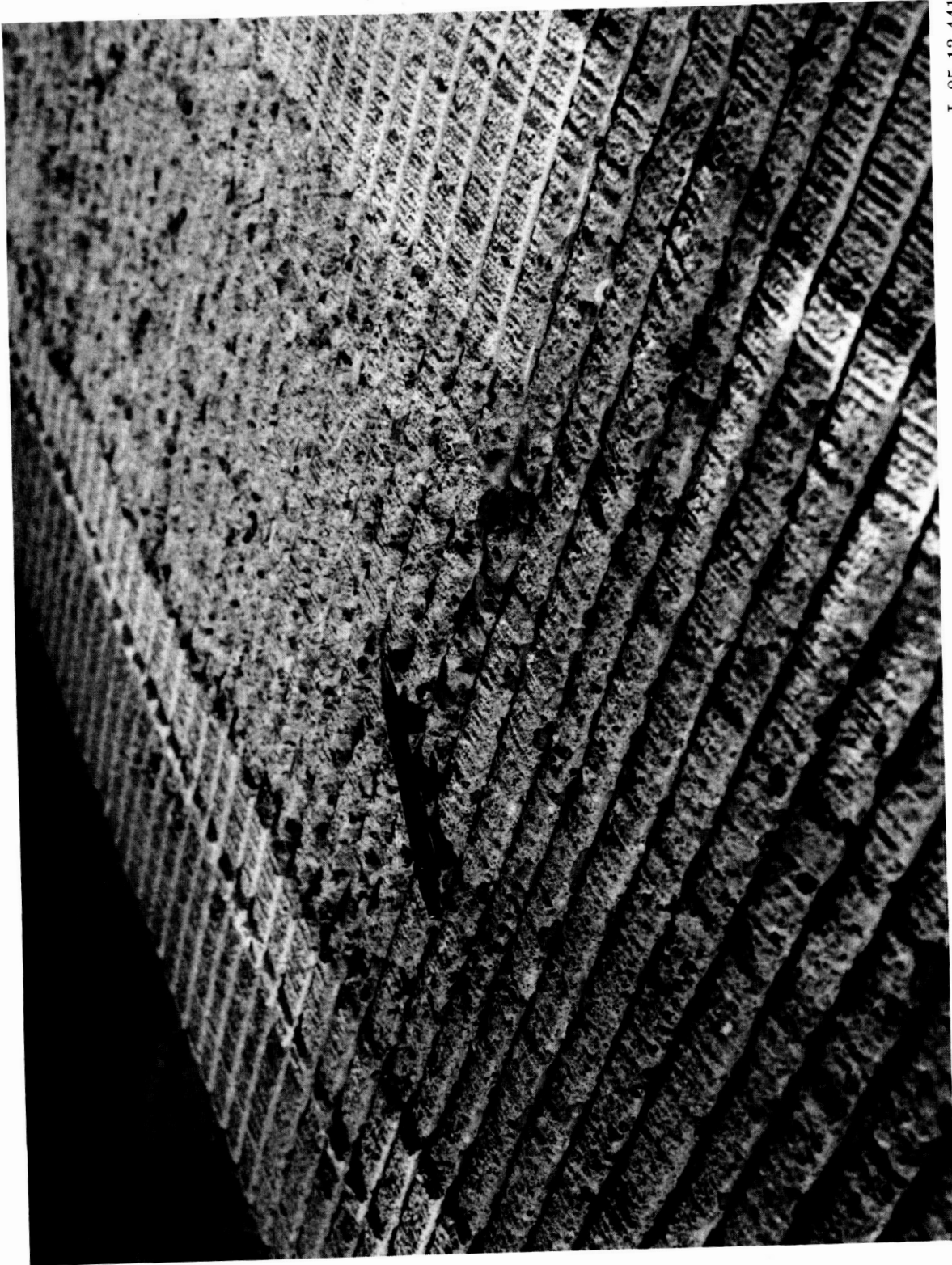
Figure A1. Comparison of side-force coefficient on various surface types and conditions. Speed, 200 knots; vertical load, ≈55 000 lb; yaw angle, 4°; tire pressure, 315 psi.

Figure A2. Painted rough surface.

Figure A3. Sandblasted rough surface.

L-85-13,441

References

1. Vogler, William A.; and Tanner, John A.: *Cornering Characteristics of the Nose-Gear Tire of the Space Shuttle Orbiter*. NASA TP-1917, 1981.
2. Davis, Pamela A.; Stubbs, Sandy M.; and Tanner, John A.: *Aircraft Landing Dynamics Facility, A Unique Facility With New Capabilities*. SAE Tech. Paper Ser. 851938, Oct. 1985.
3. Leland, Trafford J. W.; Yager, Thomas J.; and Joyner, Upshur T.: *Effects of Pavement Texture on Wet-Runway Braking Performance*. NASA TN D-4323, 1968.
4. Tanner, John A.; Stubbs, Sandy M.; and McCarty, John L.: *Static and Yawed-Rolling Mechanical Properties of Two Type VIII Aircraft Tires*. NASA TP-1863, 1981.

Table I. Summary of Test Conditions and Results

Run	Speed, knots	Yaw angle, deg	Vertical load, lb	R	Drag force, lb	Side force, lb	Drag-force coefficient	Side-force coefficient	Aligning torque, ft-lb	Overturning torque, ft-lb
1	200	0	60 900	1.00	1 000	−700	0.02	−0.01	0	900
2	208	1	66 000	1.08	1 100	4 300	.02	.07	2 200	11 100
3	201	2	65 000	1.07	1 200	9 100	.02	.14	4 100	18 700
4	206	4	66 500	1.09	1 800	15 200	.03	.23	4 200	31 500
5	195	4	59 000	.97	1 100	16 000	.02	.27	2 500	32 500
6	200	4	30 500	0.50	600	12 500	0.02	0.41	500	25 100
		4	45 700	.75	800	13 200	.02	.29	1 400	28 600
		4	53 000	.87	1 000	13 900	.02	.26	2 000	30 100
7	5	1	15 200	0.25	400	2 100	0.03	0.14	500	3 600
		1	30 500	.50	600	3 200	.02	.10	1 000	6 000
		1	45 700	.75	900	4 100	.02	.09	1 400	7 700
		1	60 900	1.00	1 400	4 300	.02	.07	2 000	8 400
8	5	2	15 200	0.25	200	4 300	0.01	0.28	700	7 600
		2	30 500	.50	500	6 800	.02	.22	1 500	12 300
		2	45 700	.75	700	8 200	.02	.18	2 500	15 200
		2	60 900	1.00	1 300	8 600	.02	.14	3 500	16 700
9	5	4	15 200	0.25	100	6 800	0.01	0.45	500	11 400
		4	30 500	.50	300	11 600	.01	.38	1 500	20 400
		4	45 700	.75	600	14 500	.01	.32	2 800	26 100
		4	60 900	1.00	1 500	15 700	.02	.26	3 900	29 300
10	5	7	15 200	0.25	100	7 600	0.01	0.50	200	13 200
		7	30 500	.50	300	14 400	.01	.47	500	25 900
		7	45 700	.75	700	18 200	.02	.40	1 300	33 800
		7	60 900	1.00	1 100	21 900	.02	.36	3 000	41 500

Table I. Continued

Run	Speed, knots	Yaw angle, deg	Vertical load, lb	R	Drag force, lb	Side force, lb	Drag-force coefficient	Side-force coefficient	Aligning torque, ft-lb	Overturning torque, ft-lb
11	5	10	15 200	0.25	0	7 300	0	0.48	100	13 000
		10	30 500	.50	100	13 600	0	.45	−200	24 700
		10	45 700	.75	300	19 600	.01	.43	0	36 800
		10	60 900	1.00	900	25 000	.01	.41	600	48 000
12	5	1	76 100	1.25	300	3 800	0	0.05	2 900	14 400
		1	91 400	1.50	1 300	2 800	.01	.03	3 100	13 600
		1	106 600	1.75	1 800	2 400	.02	.02	3 600	13 100
		1	115 900	1.90	3 400	1 800	.03	.02	3 500	12 200
13	5	2	78 200	1.28	1 100	6 800	0.01	0.09	4 700	19 100
		2	91 400	1.50	1 300	6 100	.01	.07	5 100	18 300
		2	106 600	1.75	1 800	5 400	.02	.05	6 300	17 500
		2	116 700	1.92	1 700	4 500	.01	.04	6 600	17 800
14	5	4	78 000	1.28	1 300	12 500	0.02	0.16	8 200	32 100
		4	91 400	1.50	1 600	11 000	.02	.12	9 100	30 000
		4	106 600	1.75	2 300	9 500	.02	.09	10 100	28 700
		4	118 400	1.94	2 400	8 900	.02	.08	10 400	27 000
15	5	7	76 100	1.25	1 700	22 300	0.02	0.29	7 300	51 600
		7	91 400	1.50	2 300	22 200	.03	.24	10 000	52 500
		7	106 600	1.75	4 500	20 700	.04	.19	12 100	51 000
		7	114 100	1.87	4 900	19 500	.04	.17	12 400	49 900

Table I. Concluded

Run	Speed, knots	Yaw angle, deg	Vertical load, lb	R	Drag force, lb	Side force, lb	Drag-force coefficient	Side-force coefficient	Aligning torque, ft-lb	Overturning torque, ft-lb
16	5	10	76 100	1.25	1 800	26 600	0.02	0.35	4 900	60 700
		10	91 400	1.50	2 100	27 100	.02	.30	8 400	63 100
		10	106 600	1.75	3 600	27 300	.03	.26	11 400	65 600
		10	114 800	1.89	4 800	26 600	.04	.23	12 500	65 600
17	221	0	45 700	0.75	1 000	700	0.02	0.02	200	1 800
18	220	0	45 700	.75	1 000	−600	.02	−.01	0	2 100
19	224	0	45 700	.75	1 000	0	.02	0	400	2 400

Table II. Bicubic Interpolation Equations

$$[\text{Characteristic} = \beta_0 + \beta_1 R + \beta_2 R^2 + \beta_3 R^3 + \beta_4 \psi + \beta_5 \psi^2 + \beta_6 \psi^3 + \beta_7 R\psi + \beta_8 R\psi^2 + \beta_9 R^2 \psi]$$

Coefficients of β	Cornering characteristics for—					
	F_s, lb	F_d, lb	μ_s	μ_d	M_z, ft-lb	M_x, ft-lb
β_0	−0.5996 E+04	−0.1967 E+03	0.4484 E−01	0.2396 E−01	0.2496 E+04	−0.5982 E+04
β_1	.1736 E+05	.3377 E+04	−.2305 E−01	.1362 E−01	−.1039 E+05	.1033 E+05
β_2	−.1452 E+05	−.2853 E+04	−.7313 E−01	−.2807 E−01	.1285 E+05	.1354 E+04
β_3	.3331 E+04	.8713 E+03	.4014 E−01	.9778 E−02	−.4372 E+04	−.2231 E+04
β_4	.3564 E+04	−.2888 E+03	.1481 E+00	−.7383 E−02	.1868 E+03	.5647 E+04
β_5	−.4131 E+03	.8056 E+02	−.1098 E−01	.1168 E−02	−.9751 E+02	−.6067 E+03
β_6	.5466 E+01	−.5548 E+01	.4707 E−04	−.8159 E−04	.8568 E+01	.6419 E+00
β_7	.2035 E+04	−.1618 E+03	−.5476 E−01	.4032 E−02	.8347 E+03	.4045 E+04
β_8	.1477 E+03	−.2939 E+01	.6026 E−02	−.7533 E−04	−.1449 E+03	.2728 E+03
β_9	−.1038 E+04	.1936 E+03	−.8438 E−02	−.3974 E−04	.6827 E+03	−.1740 E+04

14
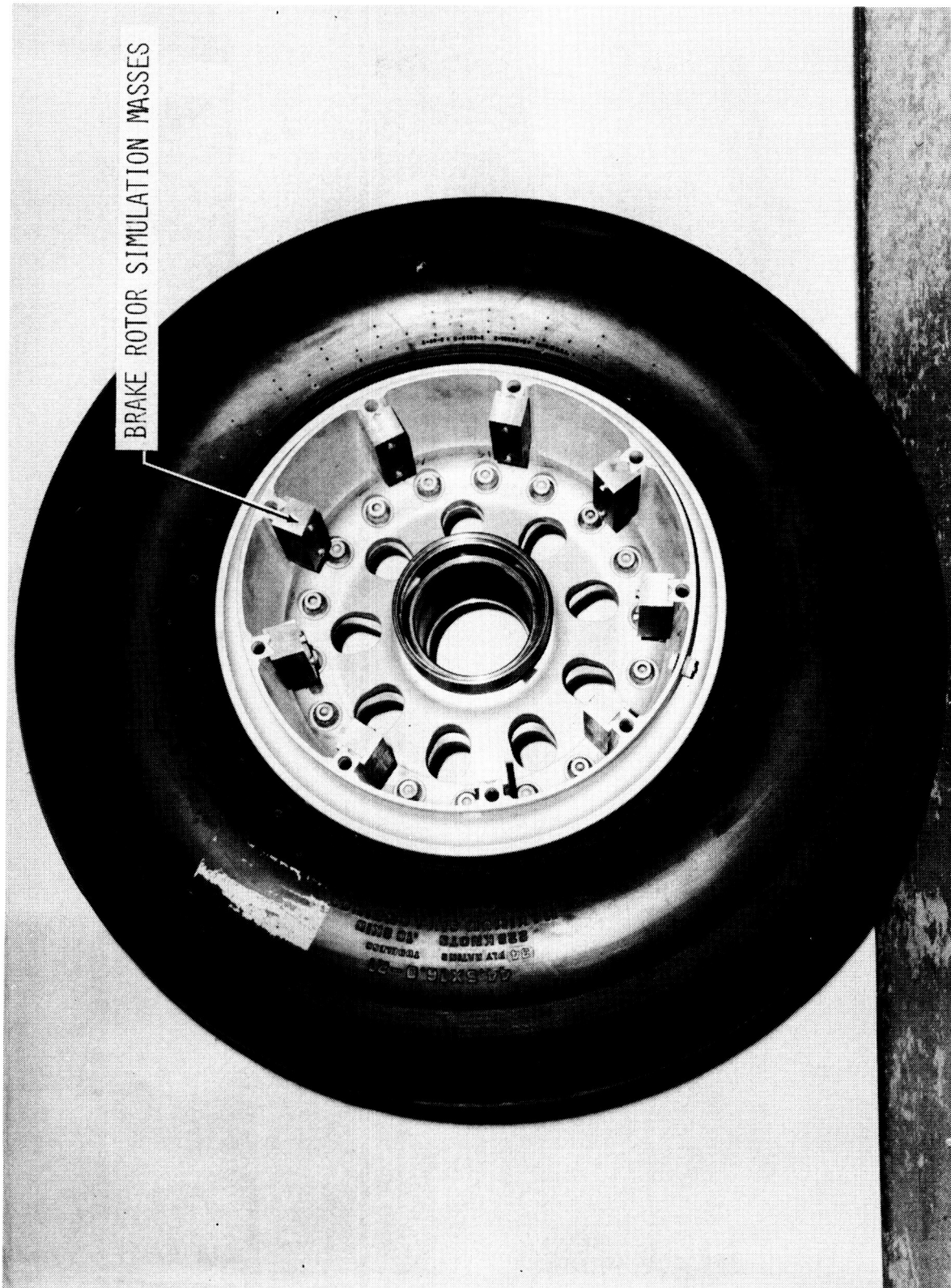
L-85-9889

BRAKE ROTOR SIMULATION MASSES

Figure 1. Main wheel and tire of Space Shuttle orbiter.
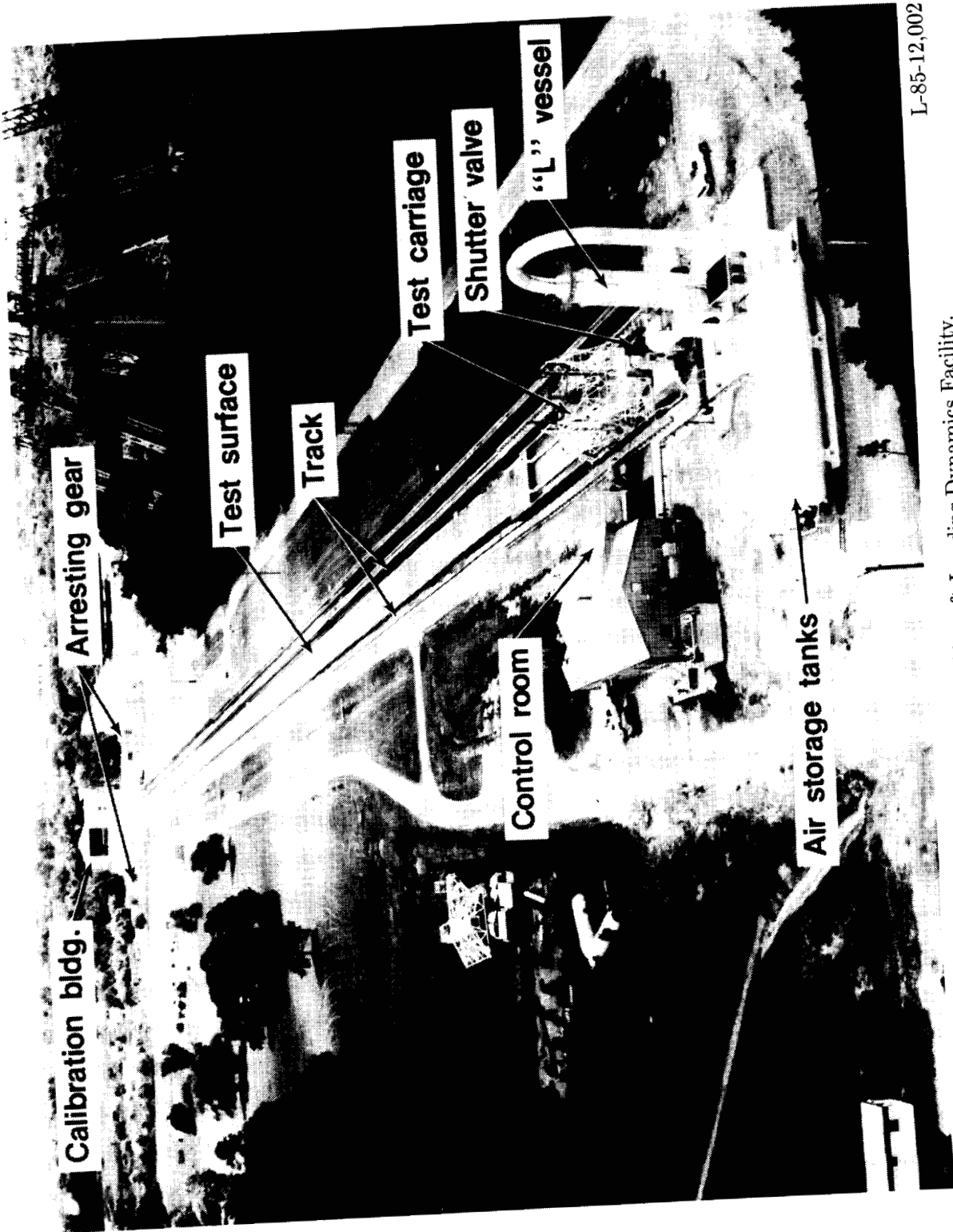
Figure 2. The Langley Aircraft Landing Dynamics Facility.

L-85-12,002
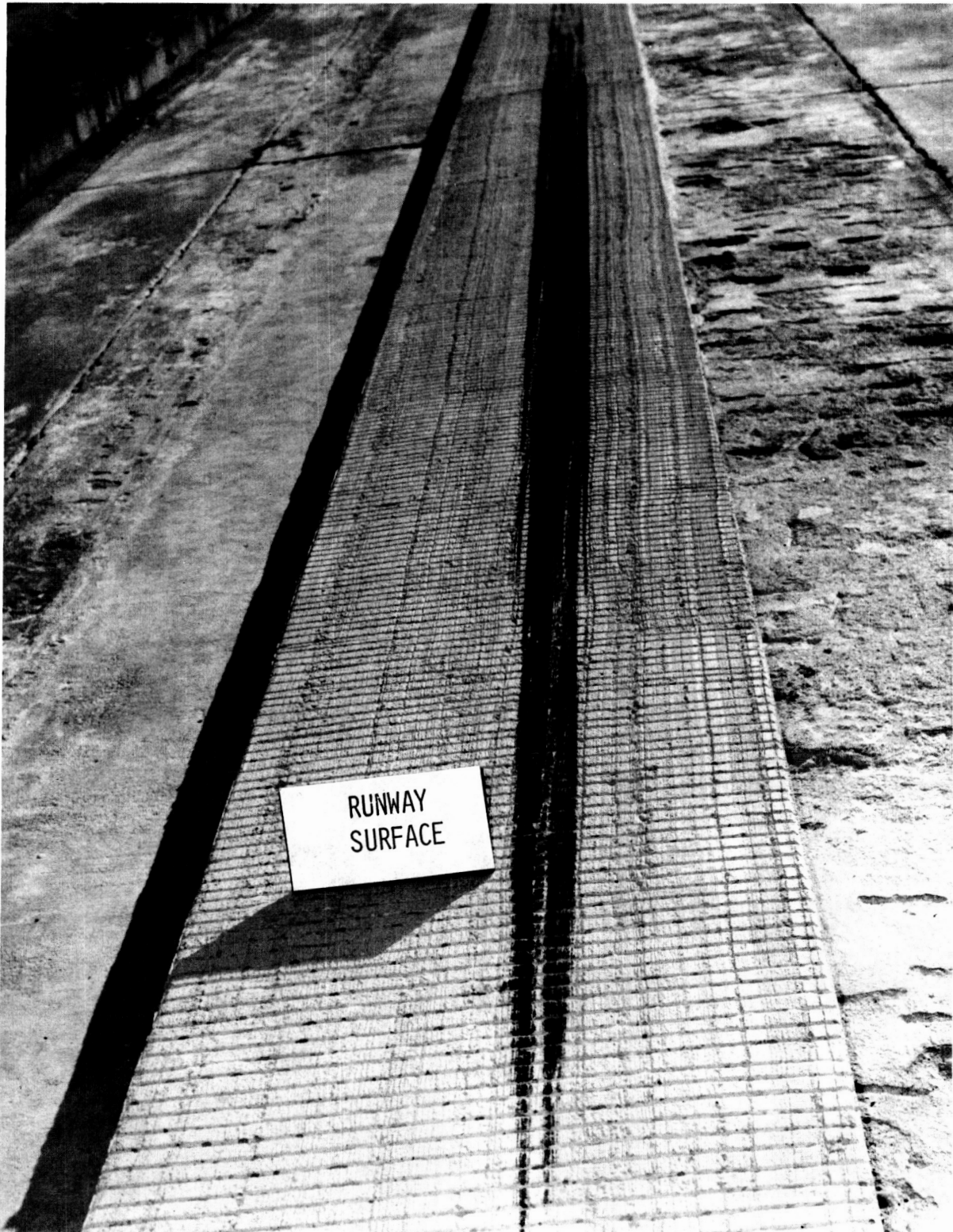
RUNWAY
SURFACE

L-85-12,239

Figure 3. Photograph of rough runway surface.
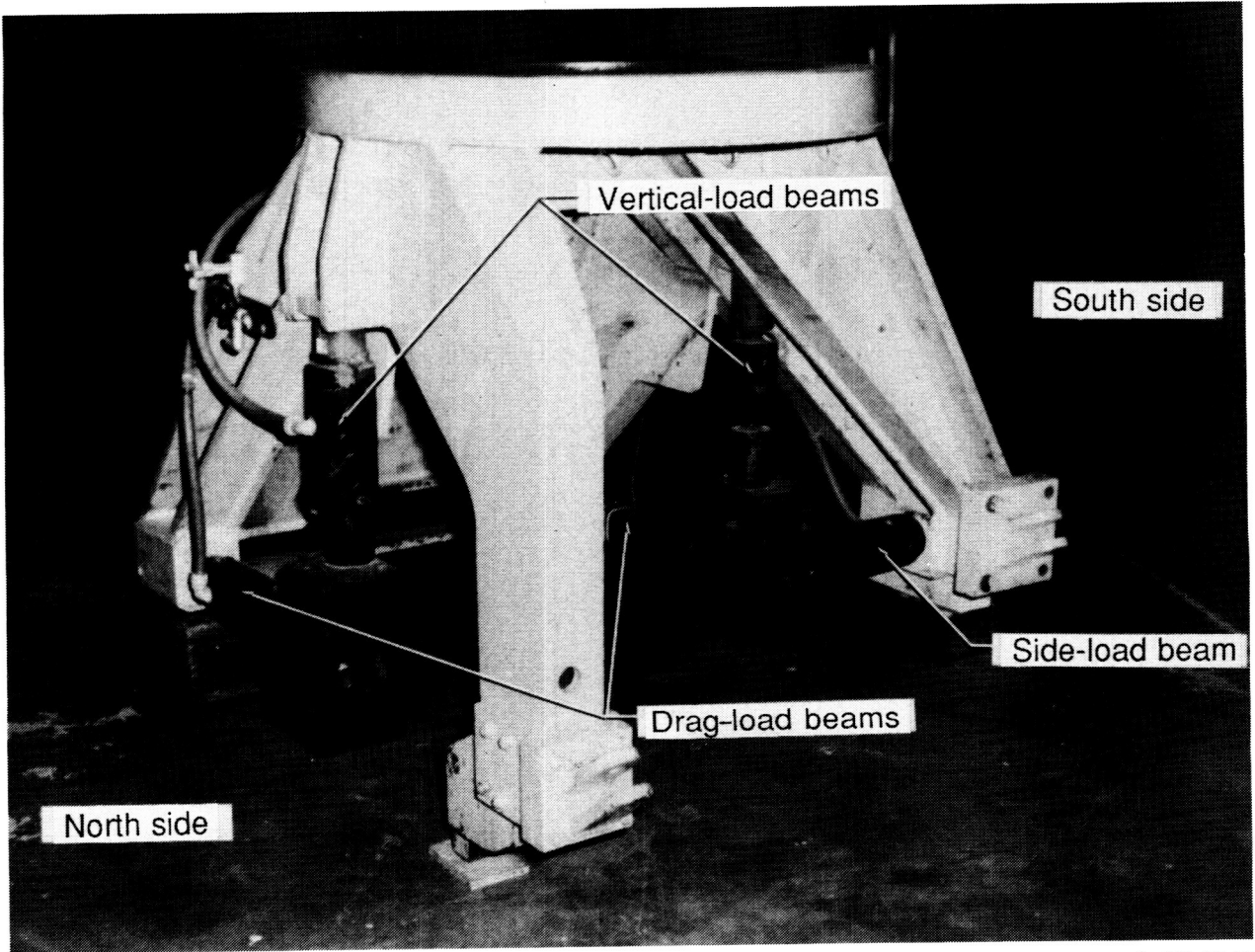
L-87-6949
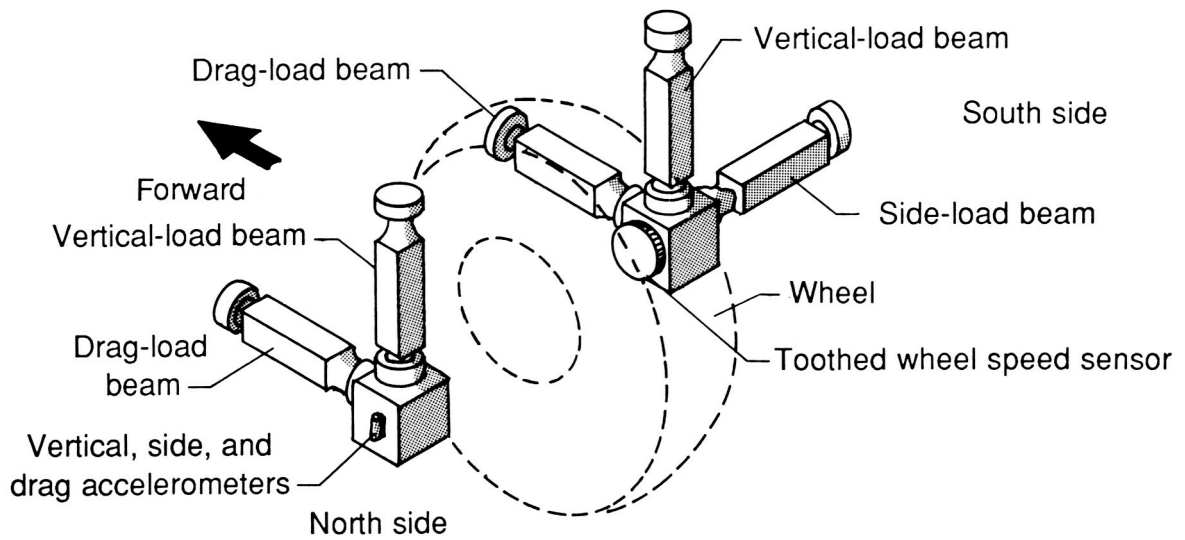
Figure 4. Photograph and sketch of dynamometer.
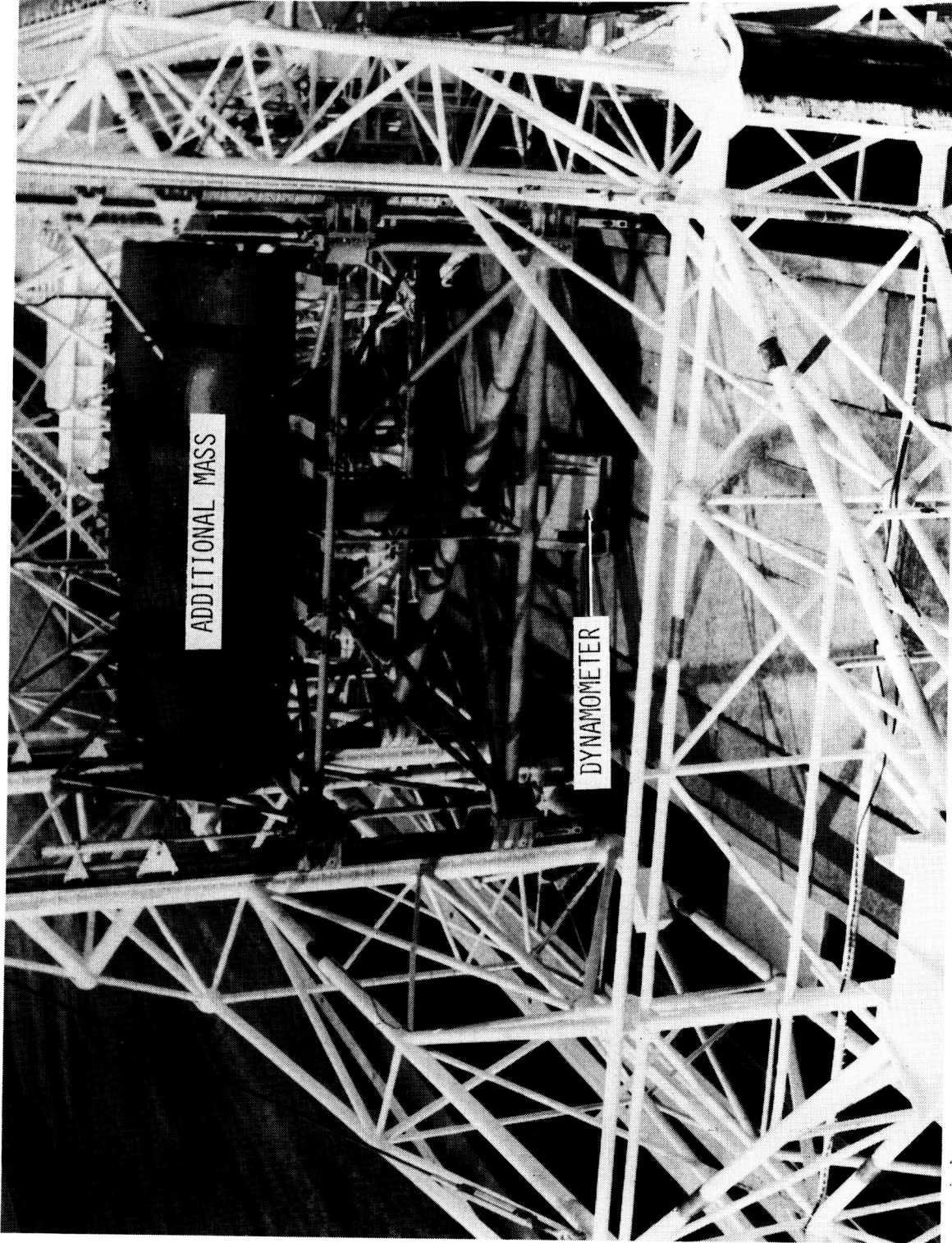
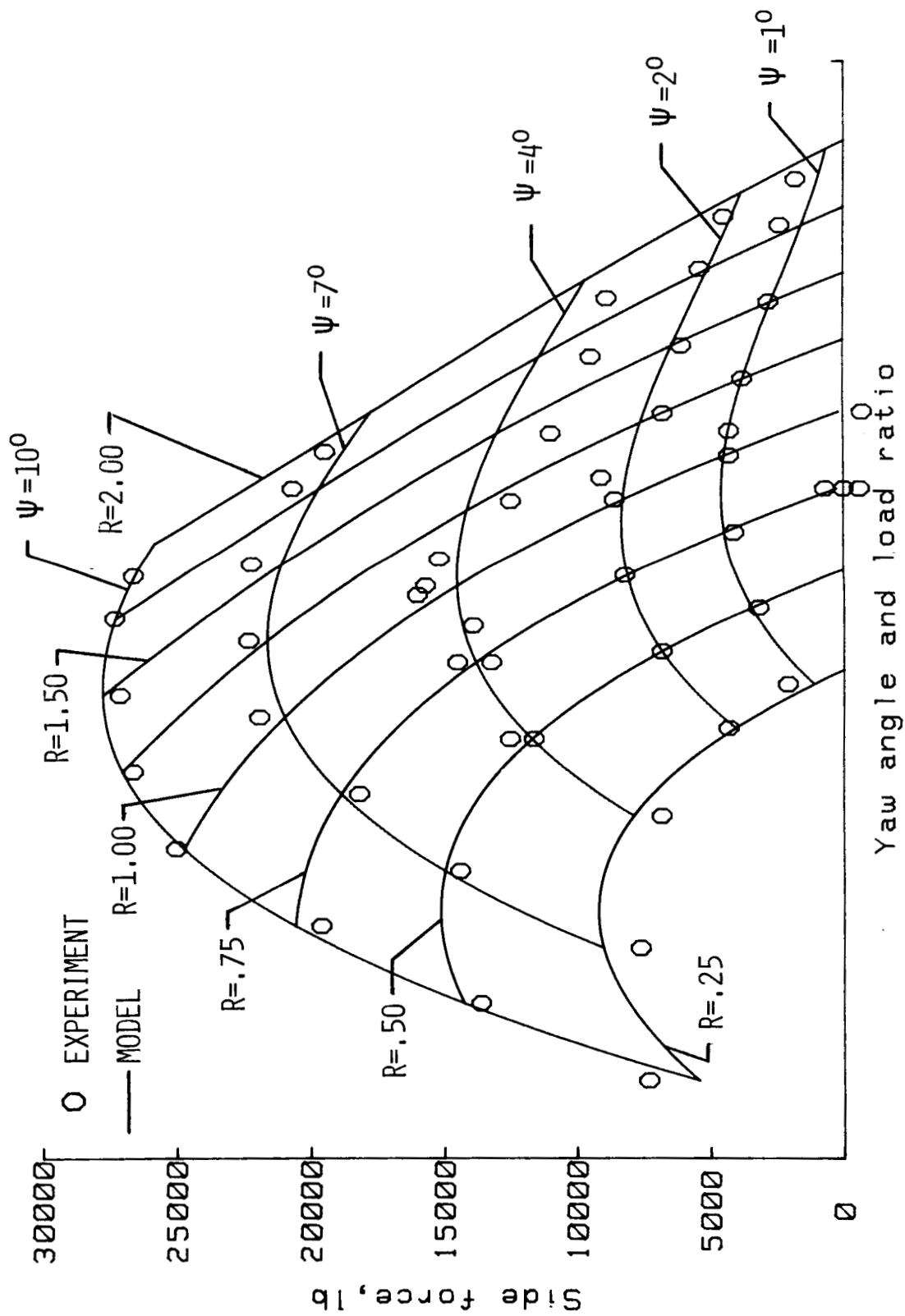Figure 5. Heavyweight towing test configuration.

L-86-11,152

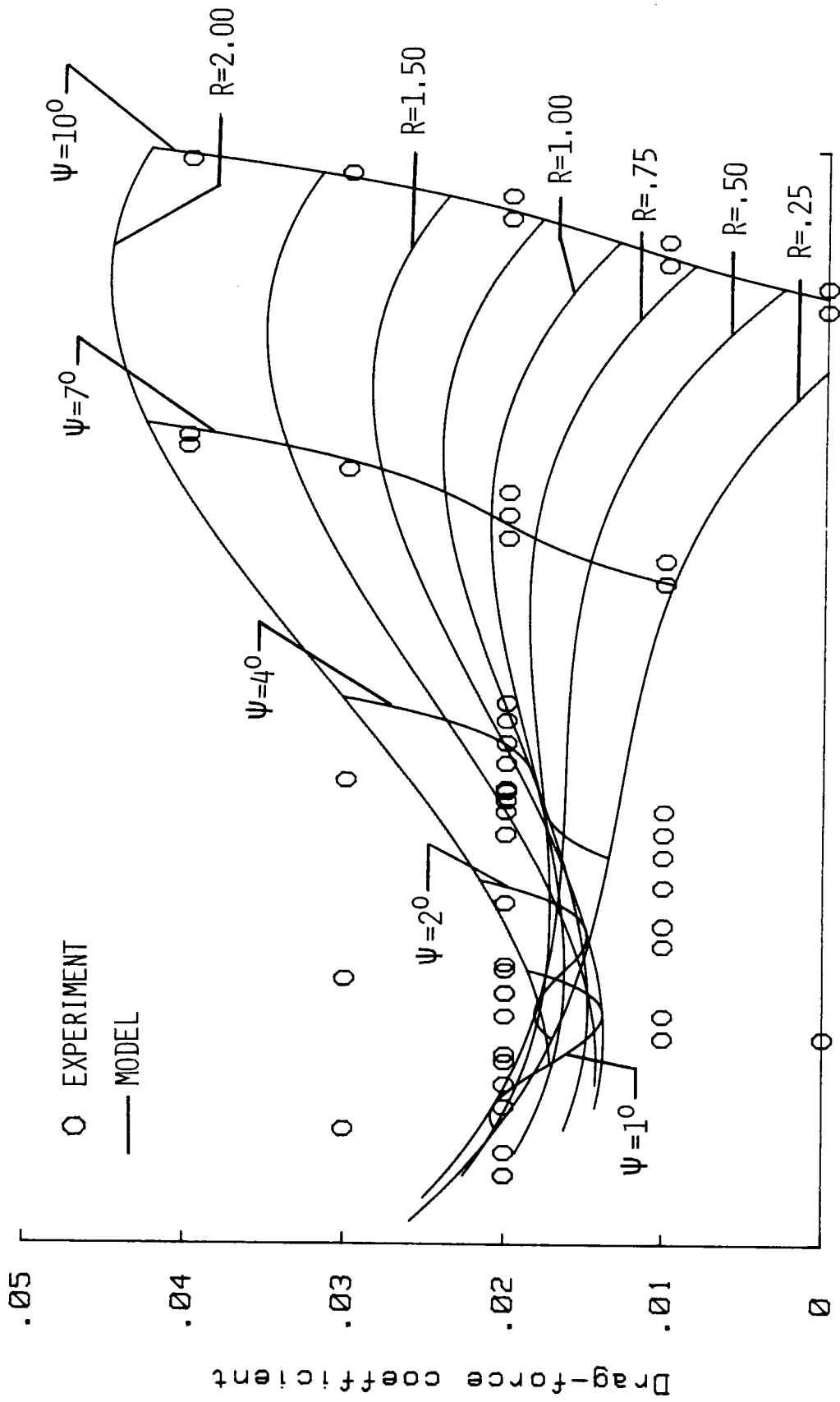Figure 6. Variation of side force with yaw angle and load ratio.
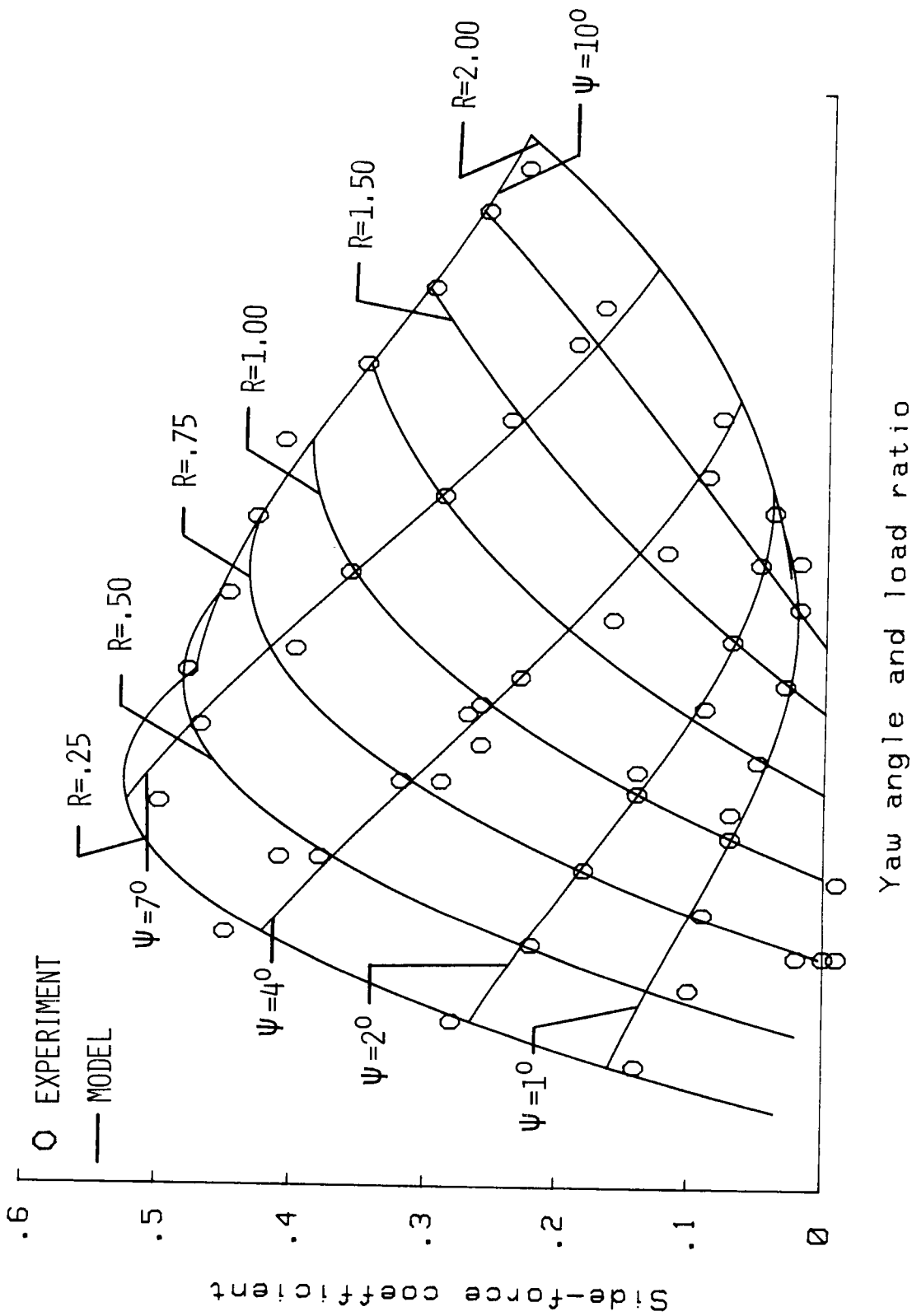
Figure 7. Variation of side-force coefficient with yaw angle and load ratio.
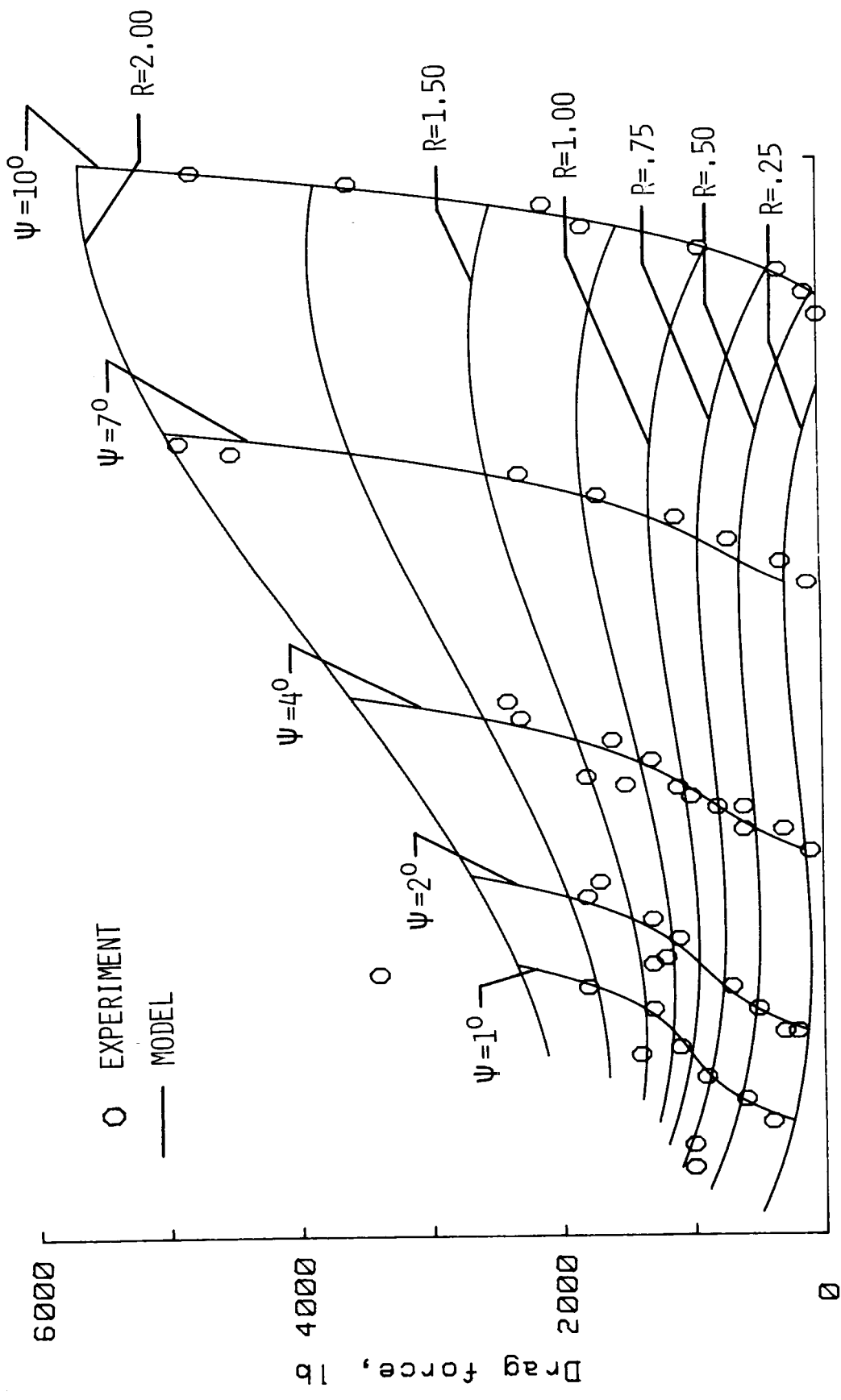
Figure 8. Variation of drag force with yaw angle and load ratio.

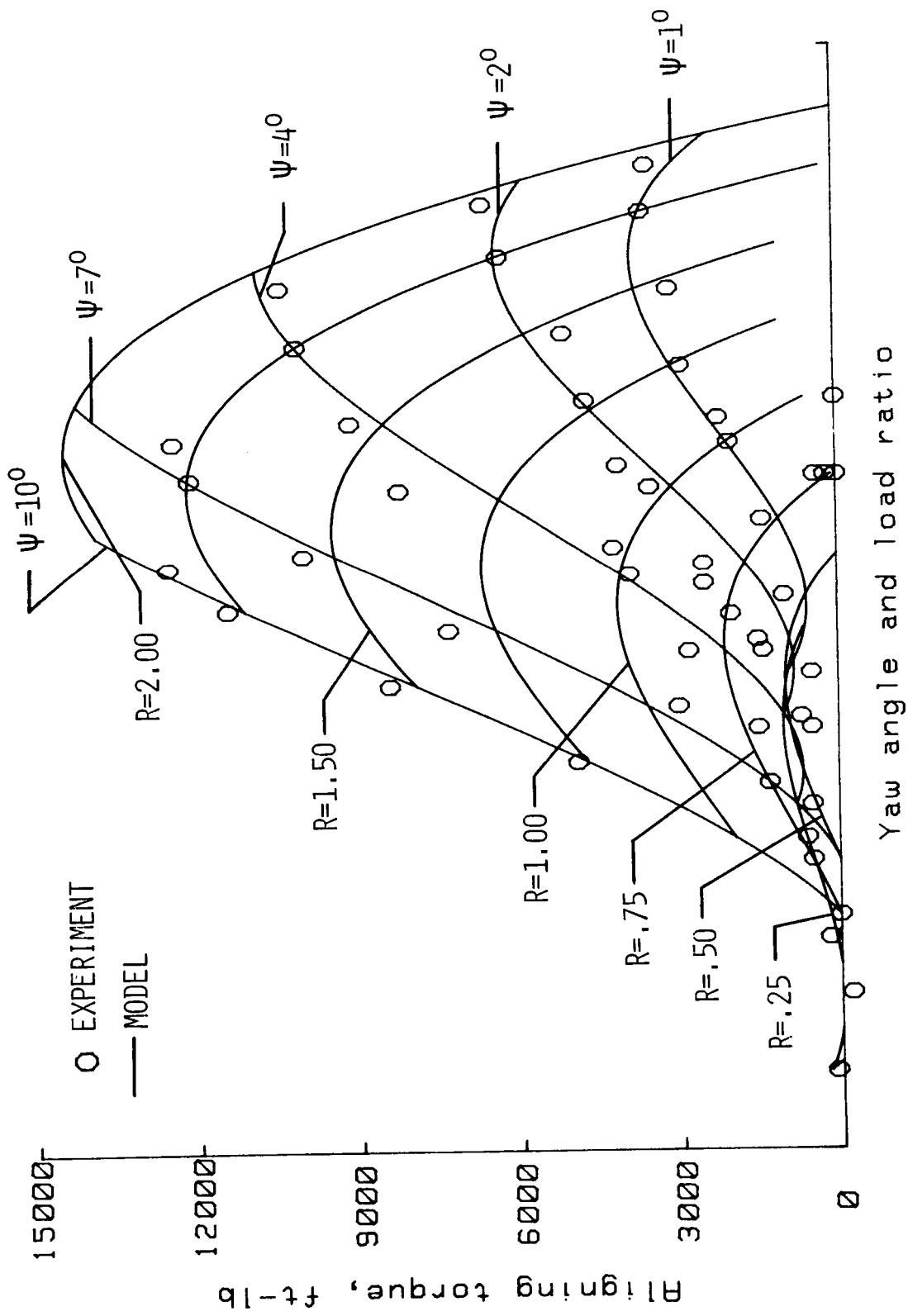Figure 9. Variation of drag-force coefficient with yaw angle and load ratio.

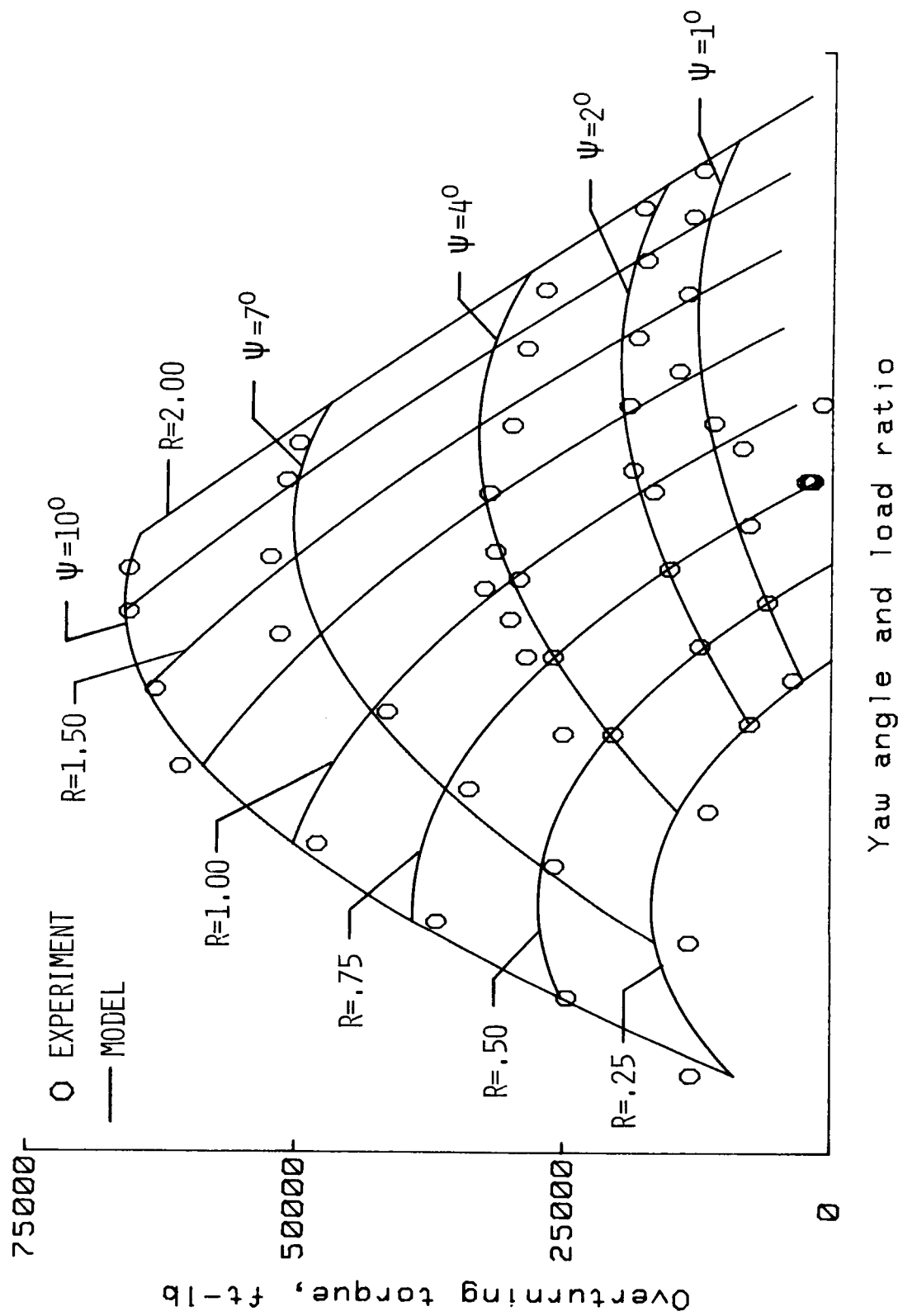Figure 10. Variation of aligning torque with yaw angle and load ratio.

Figure 11. Variation of overturning torque with yaw angle and load ratio.

NASA
National Aeronautics and
Space Administration

Report Documentation Page

1. Report No. NASA TP-2790	2. Government Accession No.	3. Recipient's Catalog No.
4. Title and Subtitle Cornering Characteristics of the Main-Gear Tire of the Space Shuttle Orbiter		5. Report Date March 1988
		6. Performing Organization Code
7. Author(s) Robert H. Daugherty, Sandy M. Stubbs, and Martha P. Robinson		8. Performing Organization Report No. L-16370
9. Performing Organization Name and Address NASA Langley Research Center Hampton, VA 23665-5225		10. Work Unit No. 551-15-01-05
		11. Contract or Grant No.
12. Sponsoring Agency Name and Address National Aeronautics and Space Administration Washington, DC 20546-0001		13. Type of Report and Period Covered Technical Paper
		14. Sponsoring Agency Code

15. Supplementary Notes

16. Abstract

An experimental investigation was conducted at the NASA Langley Research Center to study the effects of various vertical-load and yaw-angle conditions on the cornering behavior of the main-gear tire of the Space Shuttle orbiter. Measured parameters included side force, side-force coefficient, drag force, drag-force coefficient, aligning torque, and overturning torque. Side-force coefficient increased as the yaw angle was increased but decreased as the vertical load was increased. Drag force was found to increase as the vertical load was increased at constant yaw angles. Aligning-torque measurements indicated that the tire is stable in yaw.

17. Key Words (Suggested by Authors(s)) Side force Side-force coefficient Yaw angle Cornering	18. Distribution Statement Unclassified—Unlimited
	Subject Category 05

19. Security Classif.(of this report) Unclassified	20. Security Classif.(of this page) Unclassified	21. No. of Pages 26	22. Price A03